

Purdue University
Purdue e-Pubs

International Compressor Engineering Conference

School of Mechanical Engineering

2012

Thermodynamic Design of Screw Motors for Constant Waste Heat Flow at Medium Temperature Level

Jan Hütker
huetker@ft.mb.uni-dortmund.de

Andreas Brümmer

Follow this and additional works at: <http://docs.lib.purdue.edu/icec>

Hütker, Jan and Brümmer, Andreas, "Thermodynamic Design of Screw Motors for Constant Waste Heat Flow at Medium Temperature Level" (2012). *International Compressor Engineering Conference*. Paper 2132.
<http://docs.lib.purdue.edu/icec/2132>

This document has been made available through Purdue e-Pubs, a service of the Purdue University Libraries. Please contact epubs@purdue.edu for additional information.

Complete proceedings may be acquired in print and on CD-ROM directly from the Ray W. Herrick Laboratories at <https://engineering.purdue.edu/Herrick/Events/orderlit.html>

Thermodynamic Design of Screw Motors for Constant Waste Heat Flow at Medium Temperature Level

Dipl.-Ing. JAN HÜTKER^{1*}, Univ. Prof. Dr.-Ing. ANDREAS BRÜMMER²

¹ TU Dortmund, Faculty of Mechanical Engineering, Chair of Fluidics,
Dortmund, Germany
Phone: +49 231 755 – 5724, Fax +49 231 755 – 5722, E-mail: jan.huetker@tu-dortmund.de

Univ. Prof. Dr.-Ing. Andreas Brümmer
² TU Dortmund, Faculty of Mechanical Engineering, Chair of Fluidics,
Dortmund, Germany
Phone: +49 231 755 – 5720, Fax +49 231 755 – 5722, E-mail: andreas.bruegger@tu-dortmund.de

* Corresponding Author

ABSTRACT

This paper focuses on the interaction of the geometric parameters of screw motors and the fluid parameters of the system in compliance with the boundary condition of constant waste heat flow. Within the thermodynamic simulation the systematic variation of the geometric machine parameters include the number of lobes on male and female rotor and the internal volume ratio. The variation range of the system parameters consists of the dependent parameters of temperature and mass flow and of the pressure on the high pressure side of the machine. The conclusive assessment of the energetic efficiency and the operating behavior of the screw motor are demonstrated by the use of the internal power, the delivery rate and classification numbers for the inlet area and the gaps. The computed operational parameters and geometries of screw engines in applications of waste heat recovery differ significantly from the previously used machines.

1. INTRODUCTION

In addition to its classical range of use as a screw compressor, the screw machine is also used in different applications as a screw motor. The screw machine in use as a motor has its overriding application area in small and medium stationary local energy systems. In the recent past especially high-speed screw motors with small overall size continued to gain in significance. The main field of application of these machines is in systems for waste heat recovery in commercial road and rail vehicles. The energetic advantages of screw motors in comparison with alternative machine concepts are mainly based on the high overall efficiency and the good part load behavior through a wide operating range.

The geometric parameters of the machine and the properties of the working fluid have a decisive influence on the performance of the screw motor. The investigation of the influence of the geometrical parameters on the thermodynamic performance of the screw motor for specific installation conditions has been carried out successfully in the past (Brümmer and Hütker, 2011). With the restriction of constant inlet parameters in regard to pressure, temperature and mass flow, these investigations allowed fundamental technical expertise about the technical-physical loss mechanisms, the dimensioning of the machine and the efficiency of the engine. The question about the optimal combination of system and machine parameters for constant waste heat flow remained largely ignored in the past.

2. SCREW MOTOR CONSTRUCTION

The operating principle of the screw motor is based on the screw-shaped, spiral intermeshing rotors, which rotate in opposite directions inside a close-fitting housing. The gaps of the rotors, in combination with the housing, form the

working chambers. When the rotors in a displacement machine rotate, typical cyclical changes in the volume of the working chambers occur. Several operating cycles take place sequentially, during which the working chambers on the high pressure side are continually enlarged during the charging phase, while those on the low pressure side reduce in size as they are emptied. Via areas in the housing, connections between the working chambers and the inlet and outlet ports are created, according to the rotation angle of the rotors. The chambers are normally enclosed except for the rotor clearances. The rims of these apertures, those which close off the charging phase and open for the discharge phase, are referred to as control edges. The rotation angle positions of the control edges determine the internal volume changes in the working chambers.

In displacement machines, there is always an important functional separation of moving and stationary parts. The relative movement between the rotors and the internal surfaces of the housing inevitably results in gaps, which prevent mechanical friction between the rotors, and also between the rotors and the housing. There are various ways in which the gaps influence the operational efficiency and security of the machine. They are responsible for connections between the individual working areas, and between the working chambers on the low and high pressure sides of the machine respectively (Zellermann, 1996). The rotor geometry determines the length and form of the gaps.

2.1 Loss Mechanism

The description of loss mechanisms during the working cycle of a screw motor is carried out on a typical machine, selected with reference to the indicator diagram in Fig.1.

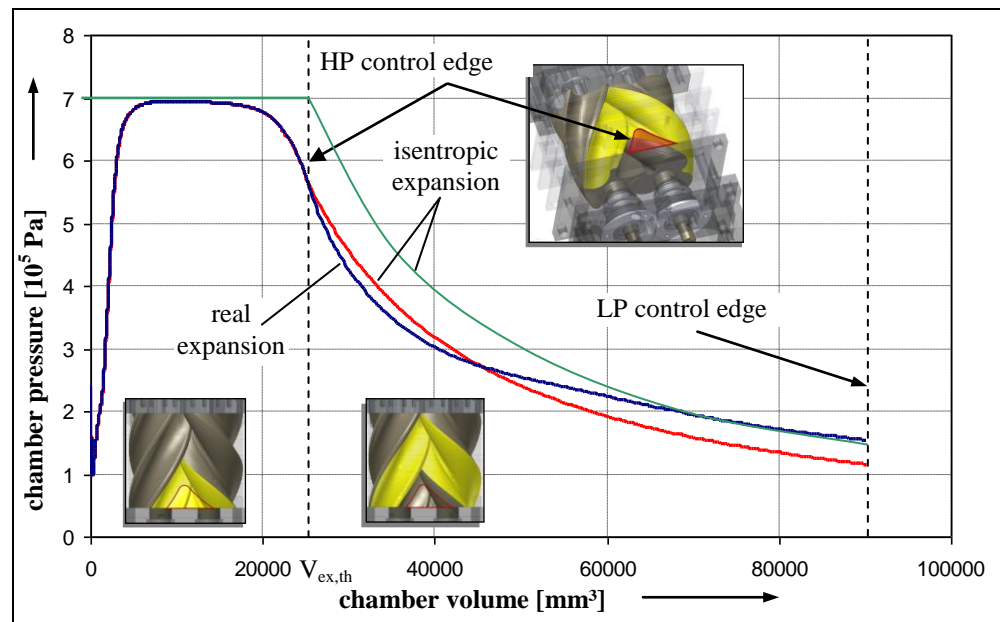


Figure 1: Chamber pressure progression dependent on chamber volume with real and isentropic charging / expansion phase. (Hütker and Brümmer, 2010)

As the inlet opening has a small area at the start of the working cycle, thus resulting in a high choking effect, maximum chamber pressure is not established instantaneously, but builds up gradually as the rotor turns. The pressure difference between the inlet pressure p_i and the chamber pressure p_c is characteristic for the charging phase. This pressure difference results from choking losses during inflow, on the one hand, and from gap mass flows, on the other hand. A further characteristic of the real charging procedure is the start of expansion before the high pressure side control edge is reached. The pressure gradient at chamber volume V_{ex} already resembles that of the first expansion phase as the control edge is reached from $V_{ex,th}$ on. The reason for the early start of real expansion is mainly the combination of continually rising chamber volume and reduction in the area of the inlet opening towards the end of the charging phase. This early start is an inherent part of the system and it also occurs in an ideal simulation, ignoring choking and gap loss factors which result from flow obstruction in the inlet cross-section.

At the start of the expansion phase the operating behavior of the screw motor is significantly influenced by the gap mass flows. In order to evaluate the influence of these flows on the energy conversion efficiency of the motor, we need to distinguish between mass flows out of the working chamber under examination and flows into it via the gap connections. Compared with isentropic expansion, the real pressure gradient during expansion is steeper at the theoretical start of expansion. The reason for this is the predominant share of mass flows out of the working chamber compared with flows into it. As the rotation angle increases, real and isentropic chamber pressures continue to converge, until, in the second phase of expansion, pressures for the real process attain higher values than those in the isentropic expansion phase. The flatter pressure curve of the real process in this area is a result of mass flows into the working chamber from the following chambers. These flows do not go directly to the low pressure side of the motor, but flow, in part, to the expanding chamber under examination, so that they apply work to the rotor flanks. The expansion phase ends when maximum chamber volume is attained. As a rule, at this rotation angle, the front flanks of the lobes cross the low pressure side control edges, and pressure equalization takes place between the working fluid and the low pressure side volume (shown isochorically in Fig.1). In the following, in order to represent the expulsion process, an idealized isochoric pressure equalization process between the chamber pressure and the ambient installation pressure at the low pressure side is assumed. The influence of the pressure difference between the end of expansion and ambient back pressure is considered below, during examination of the internal volume ratios, in connection with “over and under-expansion”.

3. PERFORMANCE DATA FOR THE EVALUATION OF THE SCREW MOTOR

In order to evaluate the energy conversion efficiency of screw motors with varying geometrical parameters, performance figures and boundary conditions have to be determined, at values for which the various different motors are comparable. Although a screw motor functions in basically the same way as a screw compressor rotating in opposite direction, both the definition of the boundary conditions and the physical description of the processes in the working chambers are more complex than in the case of screw compressors. In the following, performance figures will be defined and applied which permit both the assessment of differing rotor geometries, and the energy-based consideration of differing motor variants.

For a quantitative assessment of the gap situation and the configuration of the inlet area, the gap and inlet area value will be defined below. In contrast to flow rate and volumetric efficiency, the two previous sets of figures describe the geometric characteristics of the screw motor, and are independent on an energy-based examination of the whole working cycle. The gap value relate the fluid mass $m_{g,fill}$ to the theoretical fluid mass $m_{ex,th}$ at the start of expansion:

$$\Pi_G = \frac{m_{g,fill}}{m_{ex,th}} \quad (1)$$

The fluid mass $m_{g,fill}$ is the mass which, in the rotation angle area for charging between $\alpha_{fillbegin}$ and $\alpha_{ex,th}$, flows out of the working chamber through the time-dependent gap area of the chamber to be charged $A_G(t)$. For the gap flow, a supercritical decompression, reaching the speed of sound in the narrowest cross-section, is assumed

$$\Pi_G = \frac{\int_{\alpha_{fillbegin}}^{\alpha_{ex,th}} A_G(t) \frac{1}{\omega} d\alpha \cdot \left(\frac{2}{\kappa_i + 1} \right)^{\frac{1}{\kappa_i - 1}} \cdot \frac{p_i}{R \cdot T_i} \sqrt{\frac{2 \cdot \kappa_i}{\kappa_i + 1}} \cdot R \cdot T_i}{V_{ex,th} \cdot \rho_i} \quad (2)$$

The calculation is based on the model of a constant and isentropic gap flow through the narrowest cross-section, with negligible flow speeds before the entrance. If we assume that there is a flow blockage, the leakage becomes a function of the inlet parameters (temperature and pressure), and the time (r.p.m.), and of the geometrical and time-dependent gap area. The theoretical mass can be computed from the chamber volume at the theoretical start of expansion, and the inlet compression. It therefore depends on the inlet parameters and the geometry of the screw motor.

The inlet area value relates the mean fictive inflow speed to the speed of sound $a_i = f(p_i, T_i)$:

$$\Pi_{IA} = \frac{\bar{c}_{i,f}}{a_i} = \frac{\left(\frac{\dot{V}_c(t)}{A_{IA}(t)} \right)}{a_i} \quad (3)$$

The fictive inflow speed already used in the past (Huster, 1998), (von Unwerth, 2002) is computed on the basis of the change in the chamber volume over time, and the inlet area $A_{IA}(t)$. This means that the relationship between the mean fictive inflow speed and the speed of sound can be interpreted as a kind of mean fictive Mach number in the inlet cross-section. Analogous to the gap operating data, the inlet area data is only dependent on the geometry and the inlet parameters. A motor with low inlet area values is desirable, as this corresponds to a long charging phase and a large inlet area.

4. BOUNDARY CONDITIONS

There are numerous possibilities for the technical application of steam powered screw motors for the conversion of thermal energy of a working fluid into mechanically useful shaft power. The generable power ranges from a few kilowatts in the field of micro-cogeneration to mobile applications and solar thermal energy in the medium power range up to the industrial waste heat flow and the conversion of biomass into electricity.

The thermodynamic variation calculations presented below are carried out under the boundary condition of a constant waste heat flow. The following parameters are set for the waste gas of the waste heat source.

Waste gas temperature $\vartheta_W = 500 \text{ }^\circ\text{C}$

Waste gas mass flow $\dot{m}_W = 2000 \text{ kg} \cdot \text{h}^{-1}$

Isobaric heat capacity $c_p = 1241 \text{ J} \cdot (\text{kg} \cdot \text{K})^{-1}$

The calculation of the isobaric heat capacity occurs on the assumption of a waste gas composition consisting of 76% nitrogen, 16% carbon dioxide and 8% water. The parameters correspond to typical values in the medium power range as they occur in mobile applications in rail vehicles, in applications of cogeneration and in solar thermal energy processes. The transferring heat flow results from the product of waste gas mass flow, isobaric heat capacity and the temperature difference on both sides of the heat exchanger:

$$\dot{Q} = \dot{m}_W \cdot c_p \cdot \Delta T \quad (4)$$

The following assumptions apply to the calculation of all operating points:

Pump efficiency $\eta_p = 70 \text{ } \%$

Efficiency of heat exchanger $\eta_{HE} = 90 \text{ } \%$

Pinchpoint $\Delta T_{PP} = 10 \text{ }^\circ\text{C}$

Condensation temperature $\vartheta_{co} = 100 \text{ }^\circ\text{C}$

A screw-type motor with the following parameters is chosen as the basis for the variation of system and geometrical parameters:

Male rotor lobes $z_{MR} = 4$

Female rotor lobes $z_{FR} = 6$

Internal volume ratio $v_i = 5$

Wrap angle $\varphi_{MR} = 300^\circ$

Length/diameter ratio $L/D = 1.4$

The circumferential speed is set at $u = 100 \text{ m} \cdot \text{s}^{-1}$ and the gap heights at the housing gap, front gap and profile intermesh clearance are set at $h = 0.1 \text{ mm}$. These parameters correspond to the orders of magnitude common for dry-running screw-type machines.

The fluid parameters at the high-pressure side of the screw-type motor are determined by inlet pressure, inlet temperature and mass flow. The inlet pressure is set by the pump and, in the framework of the variation calculation, is varied between $8 \cdot 10^5$ and $24 \cdot 10^5 \text{ Pa}$. In the calculation, the pressure losses in the pipeline section are not taken into consideration. Inlet temperature and mass flow are directly interdependent. With constant waste heat flow and the known boundary conditions, the mass flow is a direct result of the selected inlet temperature. In order to limit the working area of the steam powered screw motor to the overheated area, a safety distance to the wet-steam area is kept by overheating the minimum inlet temperature by $20 \text{ }^\circ\text{C}$.

5. MODELLING AND COMPUTING

The variation calculations of the screw-motor were carried out in two independent computation steps: a geometrical abstraction and an energy-based examination. The basis of the geometrical abstraction of a screw motor is the analytical treatment of the rotor meshing. The objective of this calculation is to determine the volume curve, and to determine the inlet and outlet areas and the gap areas as a function of the male rotor angle, with preset geometrical parameters (z_{MR} , z_{MR} , ϕ_{MR} , L/D und v_i). The results of the geometrical abstraction are the basis for an energy-based examination of the operating behavior of the motor.

The computing program for the energy-based machine analysis is based mainly on mass and energy conservation. Basically, by means of a balancing process, changes in the condition of the vaporous working fluid are ascertained numerically, so that the operating behavior of the machine can be represented. This allows changes in condition in the form of rotation angle-dependent volume changes, and gap mass flows into and out of the working chamber, to be taken into account. The computational basis for process changes in the working fluid is represented with reference to the flow velocity by a zero-dimensional chamber model, which permits, in principle, the simulation of screw motors with any range of geometrical parameters.

6. SIMULATION RESULTS

In the first calculation step, the influence of the cycle parameters on the energy conversion quality of the screw motor at constant geometrical machine parameters is investigated. In this case, the absolute geometrical dimensions are not constant. The steam powered screw motor is scaled to the respective mass flow under the boundary condition of a constant circumferential speed of the male rotor.

6.1 System Parameters

In Fig. 2, the system mass flow and the axis-center distance of the screw motor for different inlet temperatures are represented as a function of the inlet pressure. The largest mass flows occur for minimal overheating over the whole pressure range. The mass flow decreases with increasing inlet temperature, which results from the boundary condition of a constant heat quantity. At constant heat flow, an increase in the motor inlet temperature is always accompanied by a reduction of the mass flow. The mass flows decreasing with increasing inlet pressure are the result of the increase in density of the working fluid. Here, the available heat quantity is not sufficient, either, to ensure a constant mass flow.

The axis-center distance is used as the measure for the design volume of the screw motor. It shows only little dependence on the inlet temperature, however decreases considerably with increasing inlet pressure. Thus the axis-center distances decreasing with increasing pressure correspond to a reduction in size of the machine subject to the determined boundary conditions.

In Fig. 3, the inlet area value and the gap value for different inlet temperatures are represented as a function of the inlet pressure. The inlet area value takes the highest values for low inlet temperatures and shows no significant dependence on the inlet pressure. The low inlet area values at high inlet temperatures can basically be explained by the temperature dependence of the sound velocity and the slightly larger design volume of this machine. The increase in the sound velocity results in a decrease in the area of the blocked flow at the beginning and towards the

end of the filling process. Due to the demand for constant circumferential speed, the axis-center distance which decreases with the inlet pressure requires an increase in speed. This results in a reduction of the filling time unfavorable for the inlet area, which, however is compensated by the improved ratio of inlet area and chamber volume. The gap value takes its maximum for high temperatures and high inlet pressures. At constant inlet pressure, the sound velocity, which increases with the temperature, encourages the detrimental gap mass flows which accounts for the energetically unfavorable character. The increasing gap values at increasing inlet pressure can be explained by both higher gap pressure ratios and decreasing axis-center distances. In case of small machines, the unfavorable ratio of chamber volume and gap area can no longer be compensated by an increase in speed.

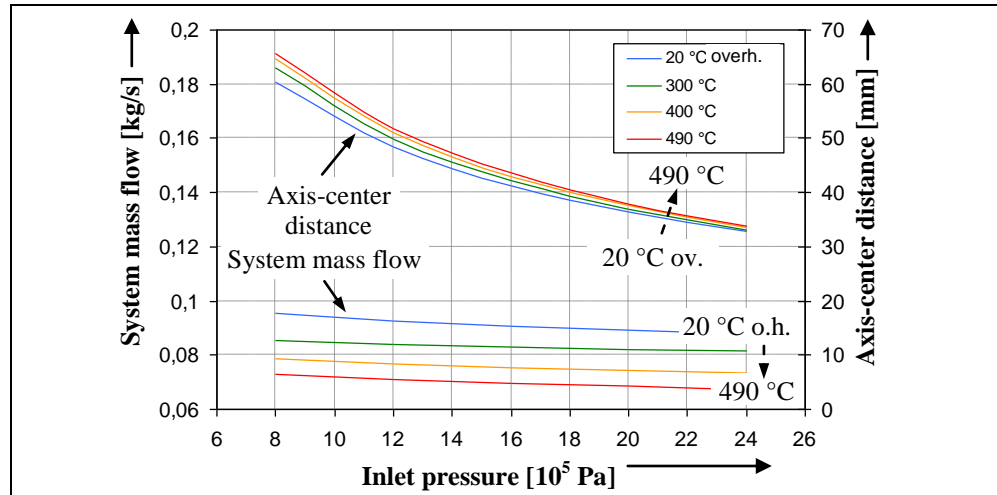


Figure 2: System mass flow and axis-center distance as a function of the inlet pressure for different inlet temperatures and constant geometrical parameters

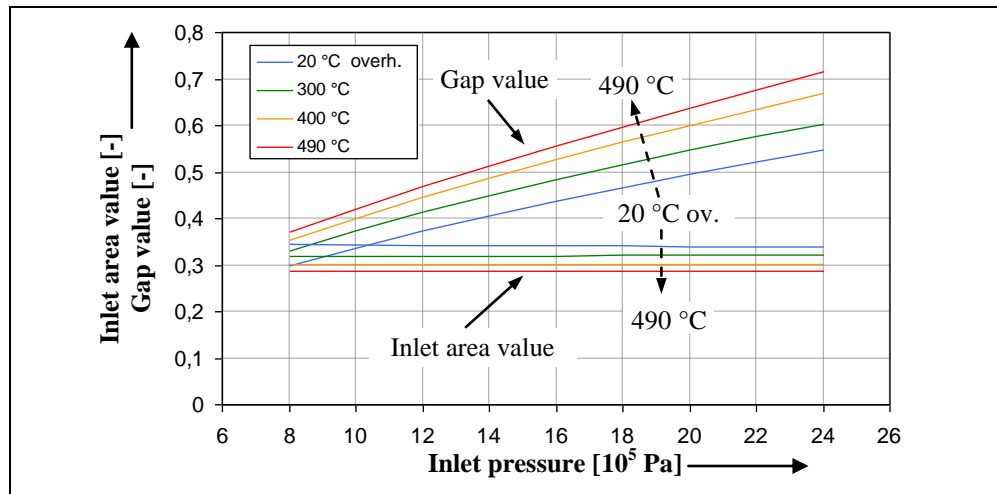


Figure 3: Inlet area value and gap value as a function of the inlet pressure for different inlet temperatures and constant geometrical parameters

Volumetric efficiency and internal efficiency rating serve the description of the energy conversion quality and are represented in Fig. 4 for the known temperatures as a function of the inlet pressure. The volumetric efficiency as a ratio of the conveyed and the theoretically possible mass flow increases with the inlet pressure and reaches the highest values at high inlet temperatures. The temperature and pressure dependence of the volumetric efficiency can be explained with reference to inlet area and gap value. An increase in the inlet temperature causes an improvement of the chamber filling (inlet area value), which, in case of constant inlet pressure, could account for the higher volumetric efficiencies at high temperatures. The volumetric efficiencies, which clearly exceed the value of $\lambda_L = 1$ along with the inlet pressure, are a result of the increasing gap mass flows for these operating points.

The internal efficiency rating - as the ratio of inner working area and ideal working area (isobaric chamber filling, isentropic expansion, isochoric pressure equalization down to low pressure and isobaric discharging) - of a machine with identical displaced volume takes the highest values for maximum temperatures in the area of high inlet pressures. The internal efficiency rating cannot be completely explained by the two values. The positive influence of a high inlet temperature on the energy conversion quality, which has already been discussed, is also reflected by the internal efficiency rating. The small internal efficiency rating in the range of small inlet pressures are the result of strong overexpansion and diminishing refill.

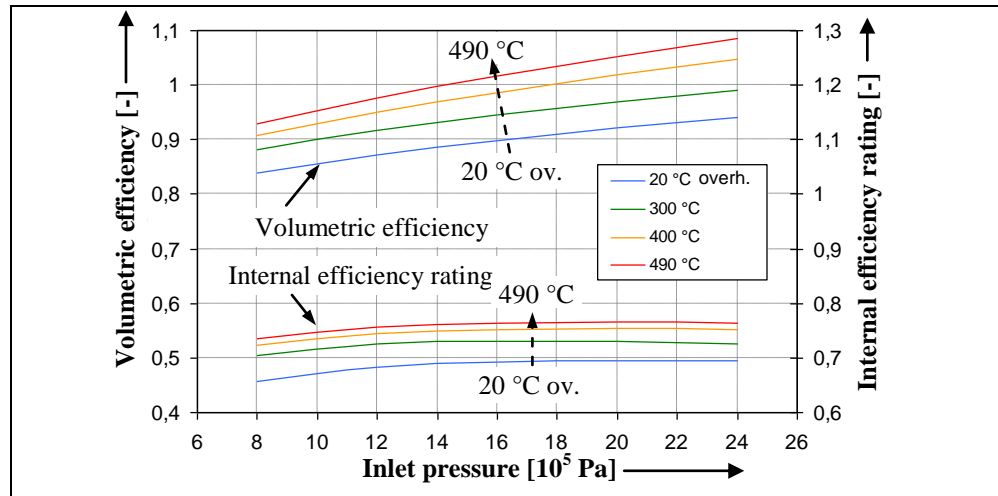


Figure 4: Volumetric efficiency and internal efficiency rating as a function of the inlet pressure for different inlet temperatures and constant geometrical parameters

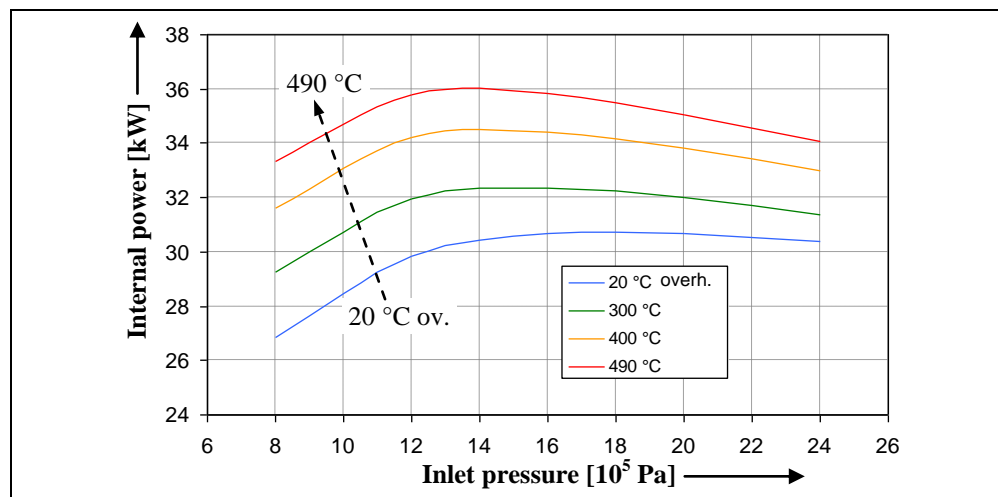


Figure 5: Internal power as a function of the inlet pressure for different inlet temperatures and constant geometrical parameters

The impacts of different inlet temperatures and pressures on the internal power of screw motors with constant geometrical values are shown in Fig. 5. High inlet temperatures and medium inlet pressures are to be expected in view of the maximum powers that can be generated. The positive effects of high inlet pressures have already been explained, whereas the power maximum in the medium pressure range is basically explained by the selection of the internal volume ratio. In the area of low inlet pressures, the selected internal volume ratio results in an overexpansion and the respective increase in the charge cycle work. At high inlet pressures, however the integrated internal volume ratio is not sufficient to adequately reduce the given pressure level. What is obvious is the displacement of the power maximum at decreasing inlet temperatures towards higher inlet pressures which seems to be a result of the favorable gap situation of this system-motor combination.

The generable power of the screw motor is opposed by the pump power required for the compression of the water. In the minimum inlet pressure range, the pump power consumed amounts to maximum 100 watt and up to 300 watt in case of maximum inlet pressure. Due to the great difference between pump and motor power, a detailed representation is not given.

6.2 Number of Lobes

For the variation of the number of lobes and the internal volume ratio carried out below, the system conditions with maximum overheating are taken into consideration. Apart from the lobes number combination of four male rotor and six female rotor lobes already considered, two other combinations with a lobes number difference of two are investigated. Screw machines with three male and five female rotor lobes are often used in applications with low pressure differences and relatively high mass flows, as for example in mechanical supercharging systems. Five male and seven female rotor lobes however, is a combination that is often found in process gas compressors with high pressure differences.

Inlet area and gap values in Fig. 6 are represented as a function of the inlet pressure for all three lobes number combinations. Both values show a qualitatively identical dependence on the inlet pressure for each lobes number combination. The low inlet area values for machines with five male and seven female rotor lobes indicate an energetically advantageous filling situation for machines with high lobes numbers. This is opposed by large gap values of these machines, which indicates an unfavorable gap situation during the filling process.

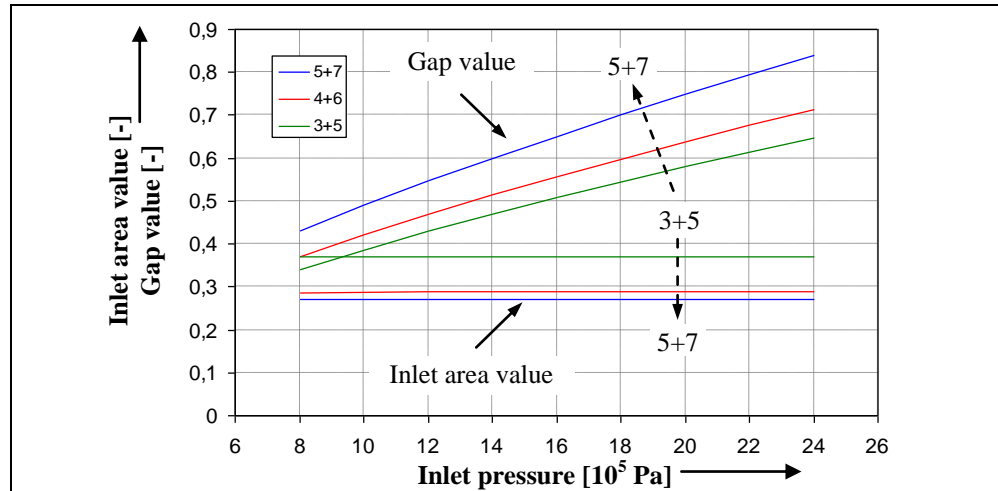


Figure 6: Inlet area value and gap value as a function of the inlet pressure for different lobes number combinations and maximum overheating

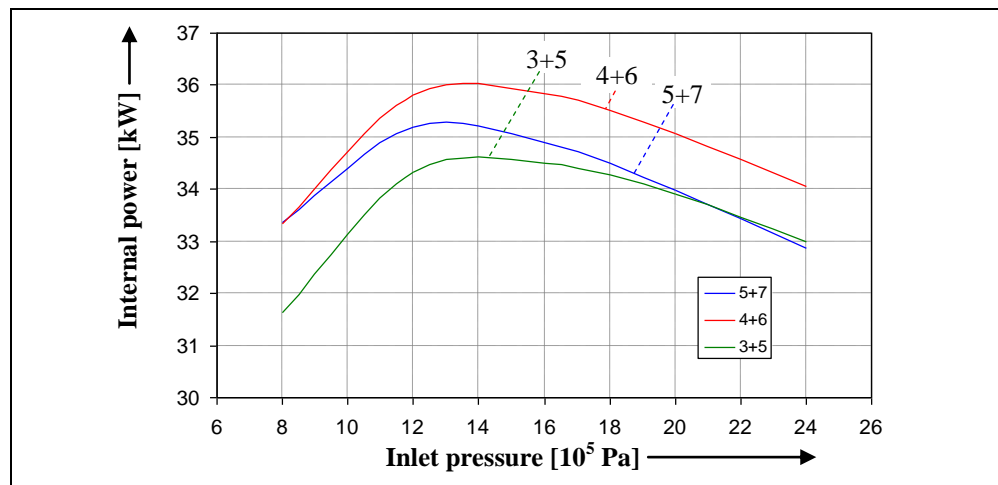


Figure 7: Internal power as a function of the inlet pressure for different lobes number combinations and maximum overheating

Fig. 7 shows the internal power of the investigated lobes number combinations as a function of the inlet pressure. For all three lobes number combinations, the pressure dependence of the internal power tends to correspond to the already known behavior.

In the area of low inlet pressures, machines with small lobes numbers (3+5) show the lowest internal powers. The main reason for this seems to be the unfavorable filling situation of this machine. Machines with 4+6 and 5+7 lobes provide comparable powers in this pressure range while the deteriorating gap situation of machines with a lobes number combination of 5+7 results in a decrease in power. The lobes number combination of four male and six female rotor lobes already investigated seems to be an energetically reasonable compromise between a still favorable filling situation, on the one hand, and moderate gap losses on the other hand.

6.3 Internal Volume Ratio

As a further machine parameter the influence of different internal volume ratios on the energy conversion quality of screw motors is thematized below. For the representation of the following simulation results, the pressure range was extended to a maximum pressure of $35 \cdot 10^5$ Pa. In Fig. 8, inlet area and gap value are shown for internal volume ratios of $v_i = 3$ to $v_i = 7$.

With a variation of the internal volume ratio, both geometrical values show the already known tendencies. The small inlet area values of machines with low internal volume ratio indicate an energetically favorable filling situation. These advantages are opposed by high gap values and the related unfavorable gap situation at small internal volume ratios.

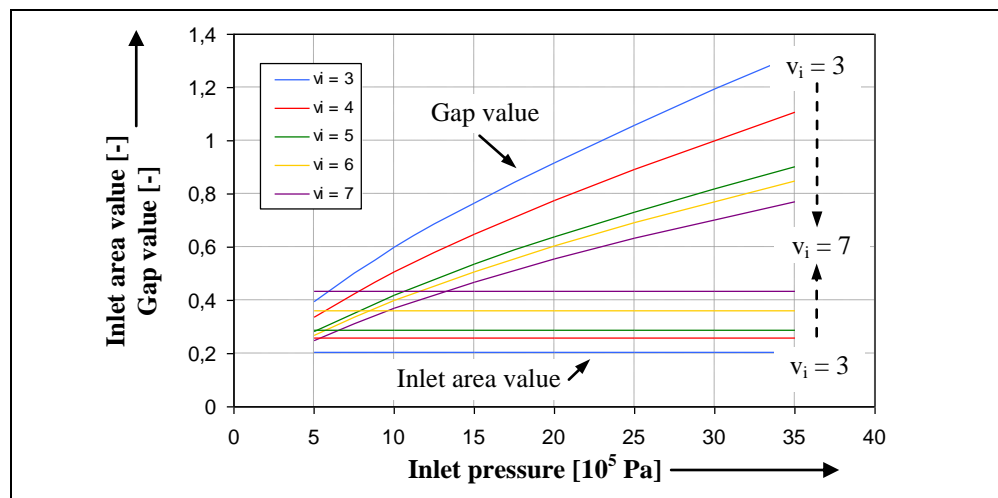


Figure 8: Inlet area value and gap value as a function of the inlet pressure for different internal volume ratios and maximum overheating

In Fig. 9, the internal power as a function of the inlet pressure is represented for the investigated internal volume ratios. In the area of small inlet pressures, screw motors with small internal volume ratio generate the highest internal power. The energetic disadvantages of screw motors with high internal volume ratio can be explained by the overexpansion which arises in the small pressure range. With higher internal volume ratios, the power maximum shifts towards higher inlet pressures. At maximum power, the screw motors operate in the range where the expansion pressure is at the level of the back pressure. An additional pressure increase results in an energetically unfavorable underexpansion, which explains the decreasing internal powers in the large pressure range. Taking into consideration the system conditions investigated here, the selection of an internal volume ratio higher than $v_i = 5$ seems to be reasonable to a limited extent only. The increasing throttling losses during chamber filling are the main reason for the stagnation of the power gain for these machines.

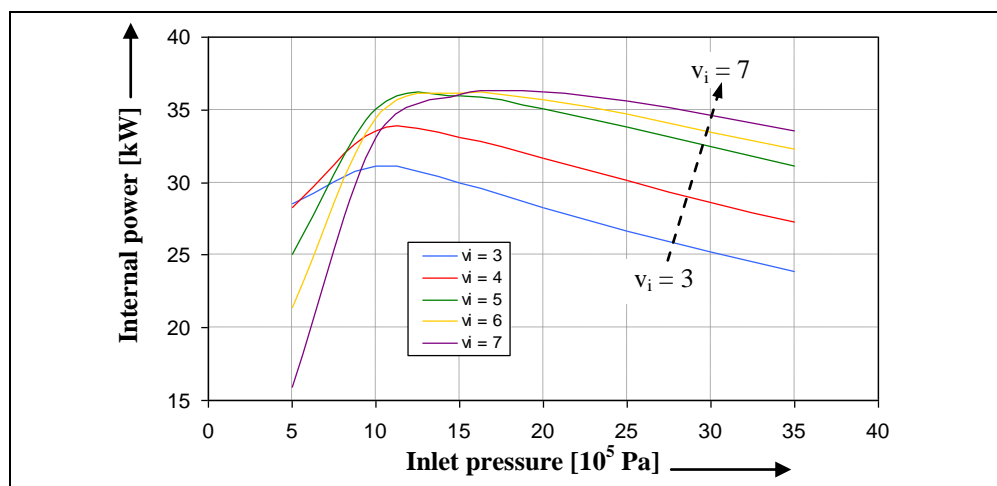


Figure 9: Internal power as a function of the inlet pressure for different internal volume ratios and maximum overheating

NOMENCLATURE

Symbol	Meaning	Dimension
A	area	(m^2)
c	flow speed	(m s^{-1})
c	chamber	(-)
co	condensating	(-)
c_p	isobaric heat capacity	($\text{J kg}^{-1} \text{K}^{-1}$)
D	diameter	(m)
ex	start of expansion	(-)
ex,th	theoretical start of expansion	(-)
f	fictional	(-)
g	gap	(-)
h	gap height	(m)
HE	heat exchanger	(-)
i	inflow/inlet	(-)
ia	inlet area	(-)
id	ideal	(-)
L	length	(m)
m	mass flow	(kg s^{-1})
n	r.p.m	(s^{-1})
p	pressure	(Pa)
P	power/performance	(W)
P	Pump	(-)
PP	pinch point	(-)
\dot{Q}	heat flow	(W)
R	gas constant	($\text{J kg}^{-1} \text{K}^{-1}$)
t	time	(s)
T	temperature	(K)
u	circumferential speed	(m s^{-1})
V	volume	(m^3)
\dot{V}	volume flow	($\text{m}^3 \text{s}^{-1}$)
W	work	($\text{kg m}^2 \text{s}^{-2}$)
W	waste gas	(W)
v_i	internal volume ratio	(-)
z	number of lobes	(-)

REFERENCES

- Brümmer, A., Hütker, J., 2011, Influence of geometric parameters on inlet losses during the filling process of screw-type motors. *Developments in mechanical engineering*, vol. 4, pp. 105-121.
- Huster, A., 1998, Untersuchung des instationären Füllvorgangs bei Schraubenmotoren. *Dissertation*, TU – Dortmund.
- Hütker, J., Brümmer, A., 2010, A comparative examination of steam-powered screw motors for specific installation conditions. 8. VDI-Fachtagung Schraubenmaschinen 2010, *VDI Bericht 2101*, S. 109-123.
- von Unwerth, T., 2002, Experimentelle Verifikation eines Simulationssystems für eine GASSCREW. *Dissertation*, TU – Dortmund.
- Zellermann, R., 1996, Optimierung von Schraubenmotoren mit Flüssigkeitseinspritzung. *Dissertation*, TU – Dortmund.